Title: Probing Axion Clouds with EHT Data Using Closure Trace Analyses

Speakers: Zhiren Wang

Collection/Series: Training Programs (TEOSP)

Subject: Other

Date: May 04, 2026 - 6:30 PM

URL: https://pirsa.org/26050052

Abstract:

Axion-like particles can form clouds around rotating supermassive black holes through superradiant instability. Via axion-photon coupling, these clouds can imprint time-dependent oscillations on the observed electric vector position angle. I will present constraints on such clouds around M87* and Sgr A* using 2017 Event Horizon Telescope polarimetric data. The analysis is based on conjugate closure trace products, which are non-imaging and insensitive to dominant calibration systematics such as station gains and polarization leakage. I will highlight the contrast between the relatively stable M87* data and the highly variable Sgr A* case, and discuss the prospects of applying this pipeline to future EHT and more sensitive next-generation EHT observations.

Probing Axion Clouds with EHT Polarimetric Data Using Closure Trace Analyses

Zhiren Wang

Based on works with **Avery Broderick**

University of Waterloo & Perimeter Institute

Grad Seminar May 04, 2026

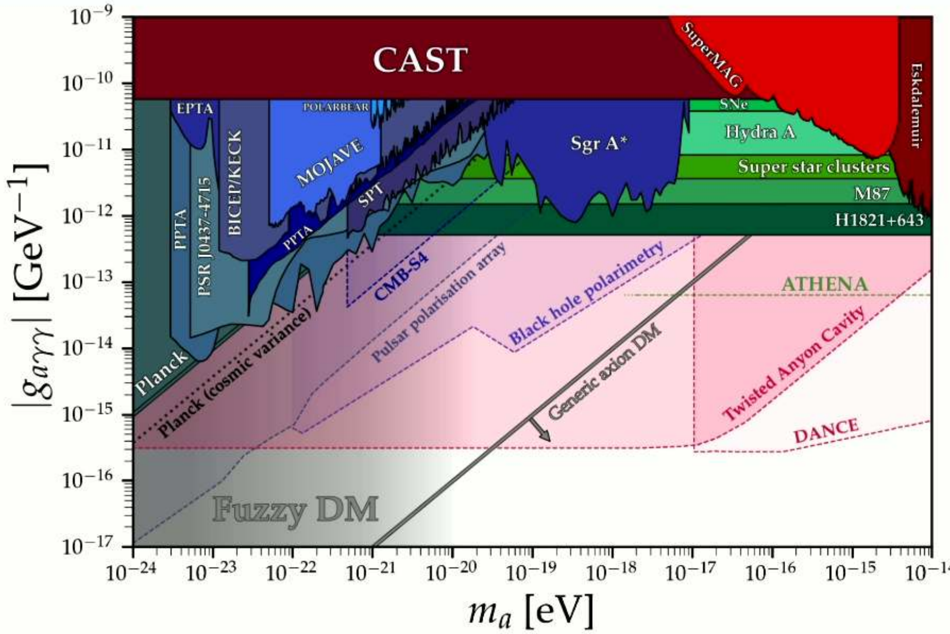

<https://cajohare.github.io/AxionLimits/docs/ap.html>

FPS N/A GPU 1 % 38 °C 6 W CPU 7 %

Roadmap

1. Motivation

Target: Axion-like particles
Mechanism: Superradiance
Observable: Oscillation in Linear Polarization

2. Method

Why the non-imaging closure trace / conjugate closure trace product for a robust search?

3. Observation

M87* as the clean test bed;
Sgr A* as the harder extension.

4. Takeaway

What the current limits mean,
and how can future observations improve the limits.

Why care about ALPs?

Theoretical Foundations

- **The Axiverse**: String theory compactifications naturally predict a vast landscape of Axion-Like Particles (ALPs).
- **Strong CP Problem**: The QCD axion remains the most elegant solution to the fine-tuning of the theta-angle.
- **Dark Matter Candidate**: "Fuzzy Dark Matter" addresses small-scale structure anomalies (Cusp-Core, Missing satellites).
- **The Detection Gap**: Masses below ~10^{-10} eV are invisible to traditional terrestrial laboratories.

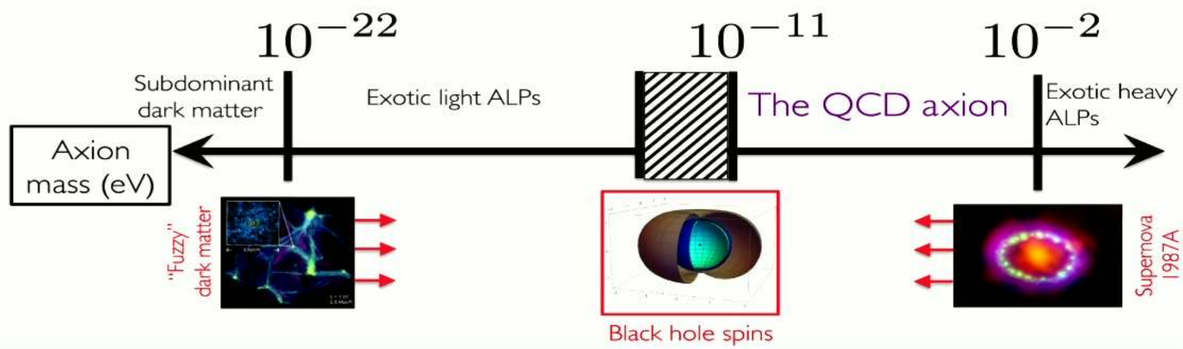

Peccei & Quinn 1977; Weinberg 1978; Wilczek 1978, Arvanitaki er al. 2009.

How to connect ALPs to SMBHs?

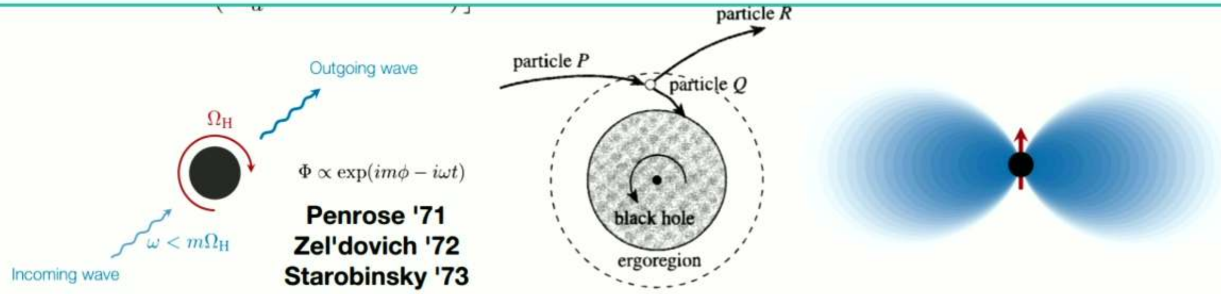

- **The idea**: The bosonic nature of axions and ALPs allows a purely gravitational, radiation enhancement process known as superradiance.
- **The trigger condition**: $\omega < m\Omega_H$
- **The mechanism**: the growth rate Γ depends on the overlap between the wave function and the ergosphere, i.e., the wavelength is comparable to r_g.
- **Quasi-Bound state**: The gravitational atom, so we can define the eigenstates (n,l,m) like hydrogen, and also the gravitational fine structure constant.
- **Consequence**: This is an exponential growth, withe the largest growth rate at n=2, l=1, m=1, forming an giant quasi-monochromatic coherent bosonic field.

$$\alpha = \frac{r_g}{\lambda_c} = \frac{GM\mu_a}{\hbar c}$$

Penrose 1971; Zel'dovich 1972; Starobinsky 1973; Arvanitaki & Dubovsky 2011; Arvanitaki, Baryakhtar & Huang 2015, Brito, Cardoso & Pani 2015.

From Coupling to Polarization Oscillation

- **The interaction**: The existence of the axion field alters the propagation properties of EM waves.
- **Axion-induced birefringence**: The LCP and RCP light has different phase velocity in an axion background, the phase difference accumulated rotates the linear polarization plane.
- **Characteristic Frequency**
- **Comparison**: This oscillation is achromatic, unlike plasma Faraday rotation $\propto \lambda^2$

$$\begin{aligned}\mathcal{L} &= \mathcal{L}_\gamma + \mathcal{L}_a + \mathcal{L}_{a\gamma} \\ &= -\frac{1}{4}F_{\mu\nu}F^{\mu\nu} + \frac{1}{2}\partial^\mu a \partial_\mu a - \frac{1}{2}m^2 a^2 - \frac{1}{4}g_{a\gamma} a F_{\mu\nu}\tilde{F}^{\mu\nu} \\ &= -\frac{1}{4}F_{\mu\nu}F^{\mu\nu} + \frac{1}{2}\partial^\mu a \partial_\mu a - \frac{1}{2}m^2 a^2 + g_{a\gamma} a \mathbf{E}\cdot\mathbf{B}\end{aligned}$$

$$\Delta\Psi = \tfrac{1}{2} g_{a\gamma} \Delta a$$

$$\omega^r_{nlm} = \mu\left(1 - \frac{\alpha^2}{2n^2} + \mathcal{O}(\alpha^4)\right)$$

$$\beta = R_M\,\lambda^2$$

Chen et al. 2022a,b, Wang & Broderick 2024.

Simulating The Orbital EVPA Pattern

- **GRRT**: To visualize the birefringence, we ray-trace the photons back to the source in the accretion disk, and modify the corresponding radiative transfer equation.
- **Parametrization**: The EVPA measurements are presented as a function of the azimuthal angle on the sky plane.
- **Definition**: “Rotativity” K, EVPA X
- **Sample movie**

$$K = -2g_{a\gamma}da/d\lambda$$

$$\chi \equiv \frac{1}{2}\arg(Q+iU)$$

$$\frac{d}{d\lambda}\begin{pmatrix}\mathcal{I}\\ \mathcal{Q}\\ \mathcal{U}\\ \mathcal{V}\end{pmatrix} = \begin{pmatrix}j_I\\ j_Q\\ j_U\\ j_V\end{pmatrix} - \begin{pmatrix}\alpha_I & \alpha_Q & \alpha_U & \alpha_V\\ \alpha_Q & \alpha_I & \rho_V + K & \rho_U\\ \alpha_U & -\rho_V - K & \alpha_I & \rho_Q\\ \alpha_V & -\rho_U & -\rho_Q & \alpha_I\end{pmatrix}\begin{pmatrix}\mathcal{I}\\ \mathcal{Q}\\ \mathcal{U}\\ \mathcal{V}\end{pmatrix}$$

$$\Delta\chi(t,\varphi,\rho) = \mathcal{A}(\varphi,\rho)\cos\left[\omega t \pm \varphi + \delta(\varphi,\rho)\right]$$

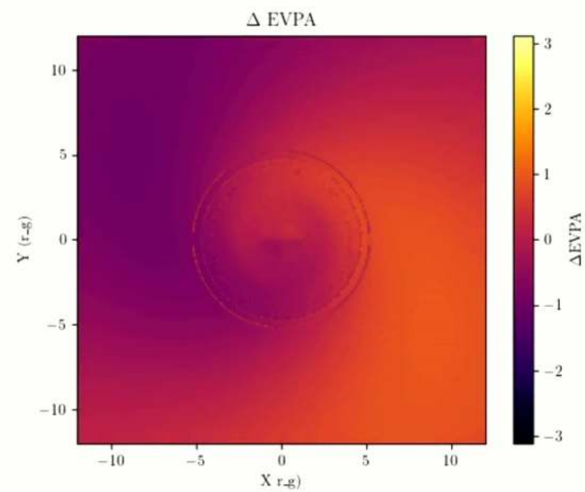

Chen et al. 2022a,b, Wang & Broderick 2026.

Why EHT? The Only Near-Horizon Polarimetric Laboratories

Observation

- **Dual-Mass Detector**: M87* (10^9 solar masses) probes ultralight bosons at 10^{-21} eV (fuzzy DM), while Sgr A* (10^6 solar masses) probes the 10^{-18} eV window.
- **Resolution**: EHT resolves horizon-scale polarized structure in the two best-observed SMBHs, allowing us to observe the densest region of the cloud, with the strongest birefringence effect.
- **Time-Domain Complementarity**: M87* has evolution timescale >> Observation window, best for phase-folding across multiple days to find weak, persistent signals. Sgr A* is a dynamic source with orbital period ~ minutes, requires a more robust analysis pipeline than M87*.

M87*

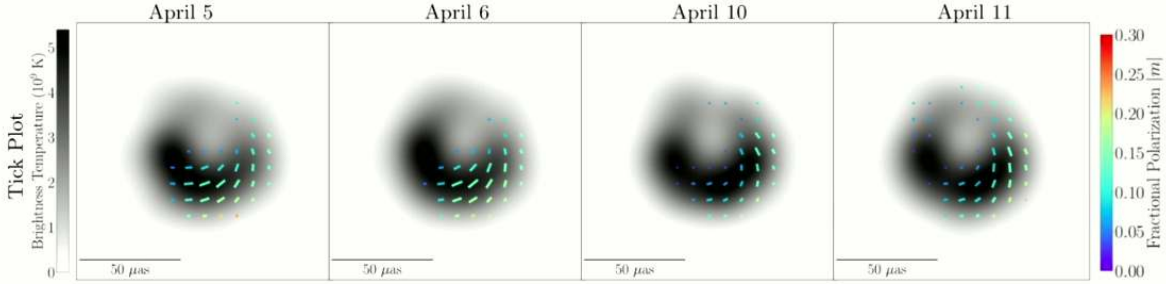

Sgr A*

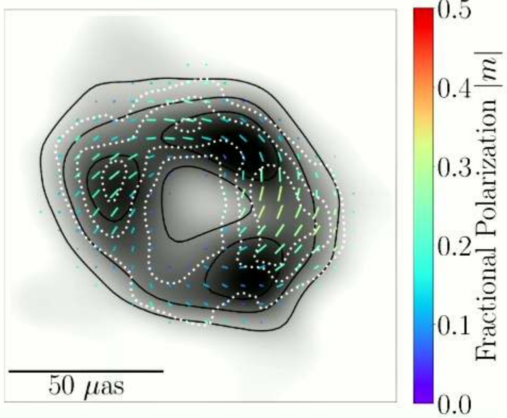

EHT Collaboration 2021 (M87* polarimetry); EHT Collaboration 2024 (Sgr A* polarimetry)

Previous Approach: Differential EVPA in the Image Domain

- **Data Foundation**: EHT Reconstructed Polarimetric Images.
- **Analysis**: To eliminate complex plasma background, they statistically evaluated the differential EVPA across two consecutive days.
- **Assumption**: The astrophysical background doesn't change in 24 hrs, while the axion signal still evolves.
- **Limitation**: Image reconstruction is a ill-posed inverse problem, subject to the sparse u-v coverage, i.e., in the Fourier domain.
- **Calibration risks**: The image quality is highly dependent on the instrumental calibrations.

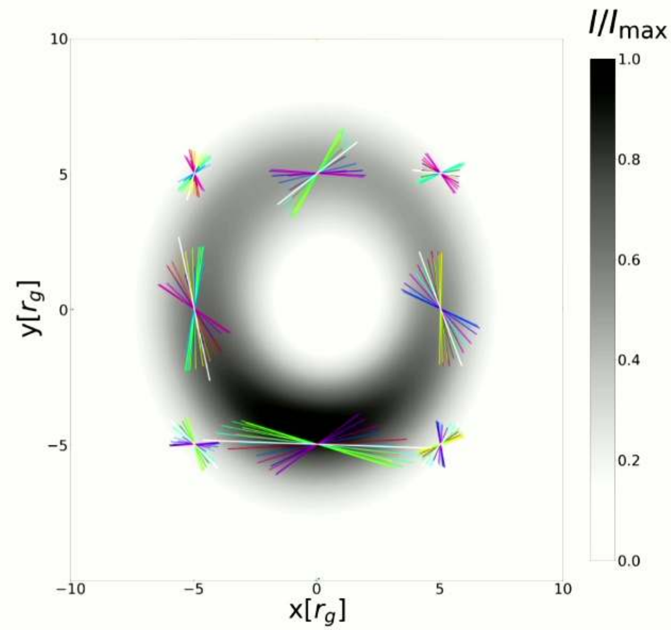

Chen et al. 2022a

Basics of Radio Interferometry

Method

Radio receivers record the electric field at each channel. In the circular-polarization basis,

$$RR_{ij} = \langle E_{R,i} E^*_{R,j} \rangle \qquad RL_{ij} = \langle E_{R,i} E^*_{L,j} \rangle$$
$$LR_{ij} = \langle E_{L,i} E^*_{R,j} \rangle \qquad LL_{ij} = \langle E_{L,i} E^*_{L,j} \rangle$$

Thus we can construct the coherency matrix

$$\bar{\boldsymbol{V}}_{ij} = \begin{pmatrix} RR_{ij} & RL_{ij} \\ LR_{ij} & LL_{ij} \end{pmatrix}$$

"Geometrical delay"

$\tau_g = \vec{b} \cdot \hat{s}/c$

Observing frequency

$\nu = \omega/(2\pi)$

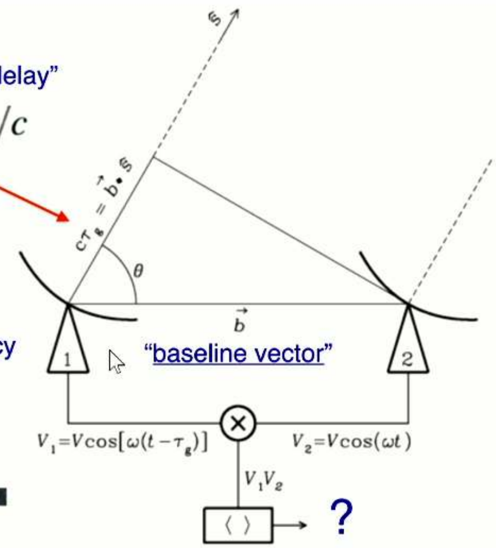

Stokes Parameters

$$I = |E_l|^2 + |E_r|^2,$$
$$Q = 2\mathrm{Re}(E_l^* E_r),$$
$$U = -2\mathrm{Im}(E_l^* E_r),$$
$$V = |E_r|^2 - |E_l|^2.$$

Radio interferometers such as the EHT measure complex visibilities at spatial frequencies set by the projected baselines b_{ij} between station i and j.

$$V_{ij} = \tilde{\mathcal{I}}(u,v) = \iint I(x,y) e^{-2\pi i(ux+vy)} dx dy$$

$$\bar{\boldsymbol{V}}_{ij} = \begin{pmatrix} RR_{ij} & RL_{ij} \\ LR_{ij} & LL_{ij} \end{pmatrix} = \begin{pmatrix} \tilde{\mathcal{I}}_{ij} + \tilde{\mathcal{V}}_{ij} & \tilde{\mathcal{Q}}_{ij} + i\tilde{\mathcal{U}}_{ij} \\ \tilde{\mathcal{Q}}_{ij} - i\tilde{\mathcal{U}}_{ij} & \tilde{\mathcal{I}}_{ij} - \tilde{\mathcal{V}}_{ij} \end{pmatrix}$$

Thompson, Moran & Swenson 2017.

Robust Observables: Bypassing Calibration with Closure Traces Method

The observed V_{AB} are generally corrupted by station-dependent gains and leakages via a sequence of linear transformations.

$$\mathbf{V}_{AB} = \mathbf{G}_A \mathbf{D}_A \bar{\mathbf{V}}_{AB} \mathbf{D}_B^{\dagger} \mathbf{G}_B^{\dagger}$$

$$\boldsymbol{G}_A = \begin{pmatrix} G_{R,A} & 0 \\ 0 & G_{L,A} \end{pmatrix},$$

$$\boldsymbol{D}_A = \begin{pmatrix} 1 & D_{R,A} \\ D_{L,A} & 1 \end{pmatrix}$$

Four-station closure trace on ABCD

$$\mathcal{T}_{ABCD} = \frac{1}{2}\,\mathrm{tr}\left(\mathbf{V}_{AB}\mathbf{V}_{CB}^{-1}\mathbf{V}_{CD}\mathbf{V}_{AD}^{-1}\right)$$

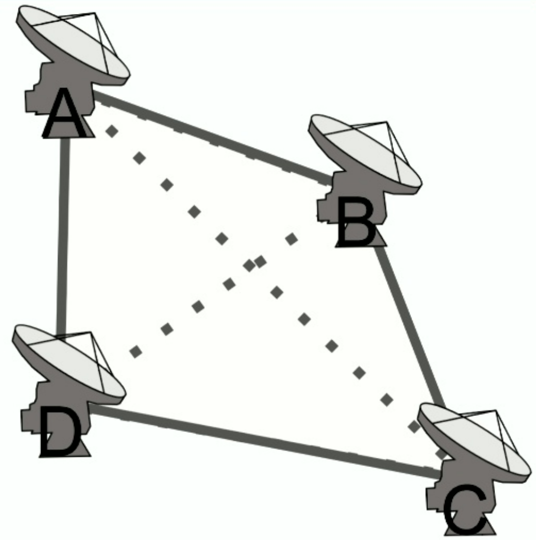

quadrangle of stations

We can show that the T is independent of the G and D

$$\boldsymbol{V}_{CB}^{-1} = (\boldsymbol{V}_{BC}^{\dagger})^{-1} = \boldsymbol{G}_B^{\dagger\,-1}\boldsymbol{D}_B^{\dagger\,-1}\bar{\boldsymbol{V}}_{CB}^{-1}\boldsymbol{D}_C^{-1}\boldsymbol{G}_C^{-1},$$

$$\mathbf{V}_{AB}\mathbf{V}_{CB}^{-1}\mathbf{V}_{CD}\mathbf{V}_{AD}^{-1} = \mathbf{G}_A\mathbf{D}_A(\bar{\mathbf{V}}_{AB}\bar{\mathbf{V}}_{CB}^{-1}\bar{\mathbf{V}}_{CD}\bar{\mathbf{V}}_{AD}^{-1})(\mathbf{G}_A\mathbf{D}_A)^{-1}$$

$$\Rightarrow \mathcal{T}_{ABCD}^{\mathrm{obs}} = \frac{1}{2}\mathrm{tr}(\mathbf{X}\mathbf{M}\mathbf{X}^{-1}) = \frac{1}{2}\mathrm{tr}(\mathbf{M}) = \mathcal{T}_{ABCD}^{\mathrm{true}}$$

T is calibration independent/insensitive to station gains and leakage while retaining full polarimetric information.

Broderick & Pesce 2020

Conjugate Closure Trace Product: Data to Be Fitted

Method

The discriminating indicators of polarization

$$\mathcal{C}_{ABCD} = \mathcal{T}_{ABCD}\mathcal{T}_{ADCB}$$

no polarized substructure $\Longrightarrow \mathcal{C}_{ABCD} = 1$

This is a non-imaging method. Unlike image-domain methods, CCTP is calculated directly from visibilities, ensuring that our search for periodic 'wiggles' is not biased by the imaging algorithm.

Closure trace removes station-based calibration terms.
CCTP = 1 when there is no polarized substructure.
So CCTP(t) is the robust time-series observable we fit.

M87* April 11, 2017

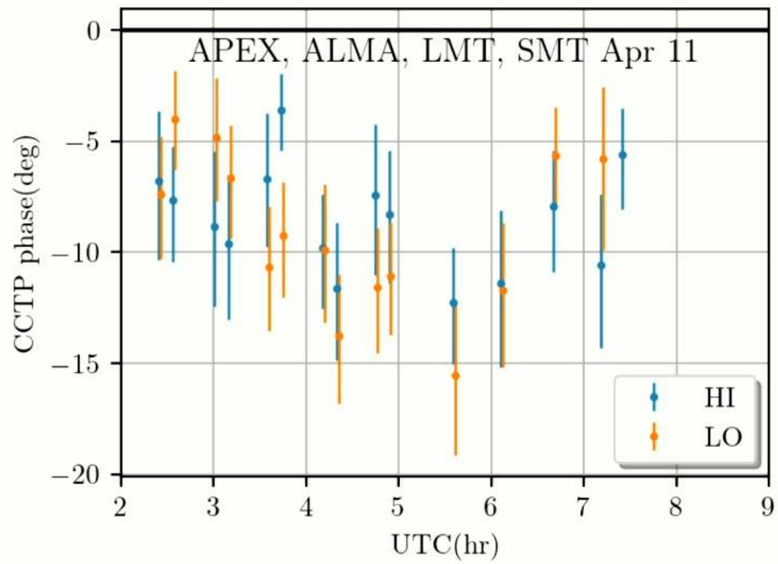

CCTP is complex, under the S/N of EHT data, the phase is more sensitive to polarized substructure than the amplitude.

Broderick & Pesce 2020; Wang & Broderick 2026a,b.

The Pipeline

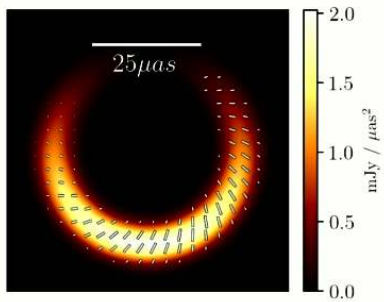

→

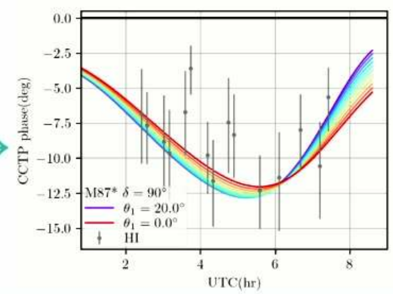

→

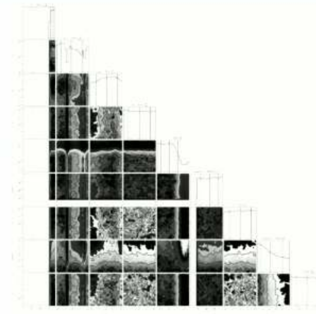

→

$$n_{\mathrm{cyc}} = \frac{\alpha c}{2\pi r_g} 24\,\mathrm{hr}$$

$$\theta_1 = \langle \mathcal{A}(\phi) \rangle_\phi = \frac{\langle \mathcal{A}'(\phi) \rangle_\phi}{2\pi} c_{a\gamma}.$$

Base Geometric Models to Simulated Movies

Simulate EHT Observations and Construct CCTPs

Robust MCMC Inference via CCTP

Connect Posteriors to Parameter Constraints via Ray-traced Movies

Axion impact can be further parametrized as

$$\theta(t,\phi) = \theta_0 + \theta_1 \cos\left[\omega(t - r_{\mathrm{ring}} \tan i \cos\phi) + \phi + \delta\right]$$

Same logic for both targets.
Sgr A* has a "mean image" alternative to the base geometric model.
Sgr A* needs detrending before the fit.

FPS N/A GPU 0% 39°C 6W CPU 6%

M87*: the clean test bed

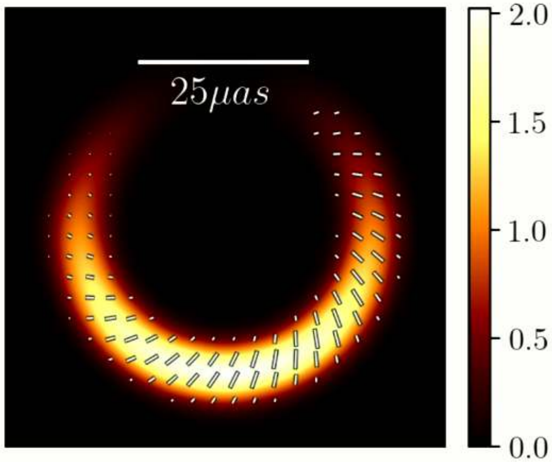

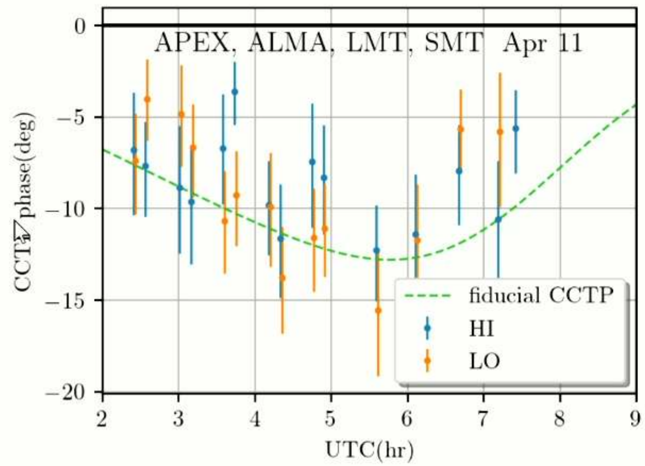

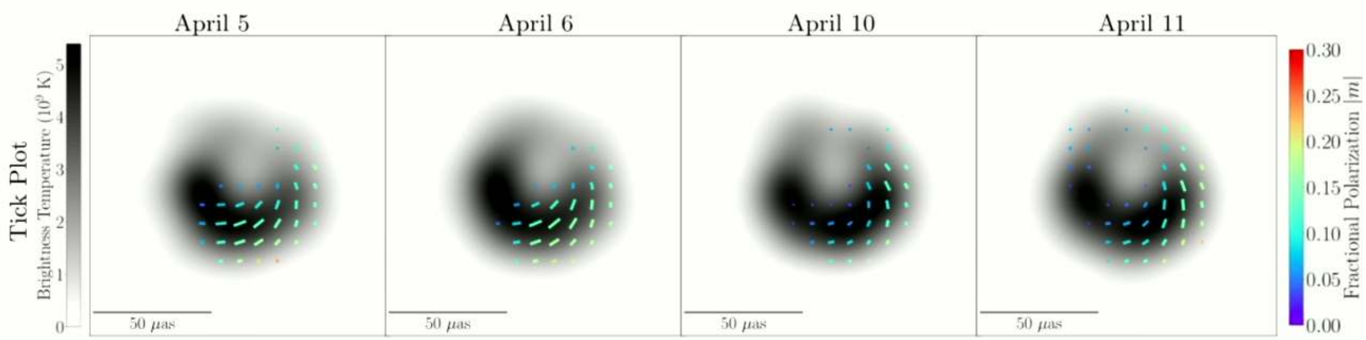

Wang & Broderick 2024; EHT Collaboration 2021.

M87* result

- We performed separate fits to Apr 5+6, 10+11, and 5+6+10+11.
- The full 2017 dataset gives the strongest bound.
- We find no robust evidence for an axion cloud in M87*, but we set a robust constraint on the ALP parameters.

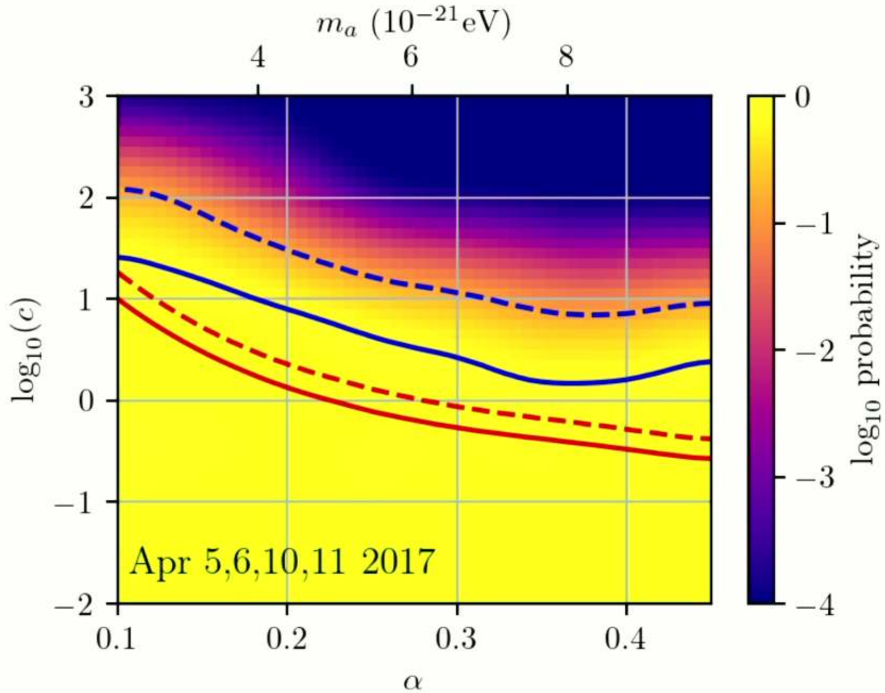

Takeaway

- M87* is where the method is cleanest: it validates CCTP as a real constraint pipeline and a viable tool for future axion searches across different mass scales.
- The limit comes from a non-imaging observable, so it is less exposed to image-domain calibration assumptions.

Wang & Broderick 2024; Chen et al. 2022a.

The Challenge of Sgr A*

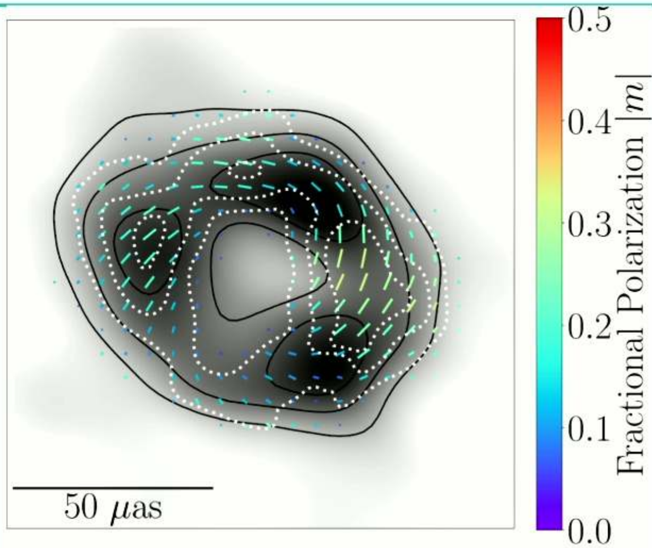

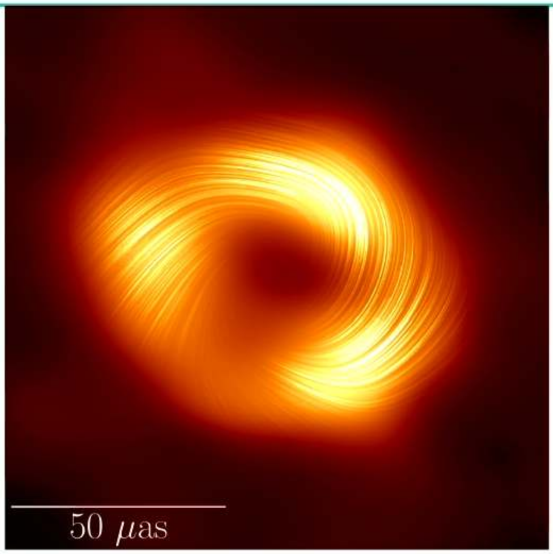

- The dynamical timescale of Sgr A* is ~ mins.
- This image is already a multi-day ensemble average of the accretion flows.
- We cannot perform a multi-day fitting, but to only focus on the best single day (April 11, 2017).
- We have to upgrade our methodology.

Wang & Broderick 2026， EHT Collaboration 2024.

FPS N/A GPU 0% 39°C 6W CPU 3%

Methodology Change for Sgr A*

- **Base Astrophysical Model**
  - A geometric model like M87*
  - A reconstructed polarimetric image + Parametrized EVPA Oscillation
- **The Detrending Procedure**
  - We interpret much of this variability as intrinsic astrophysical variability of the source rather than as evidence for the coherent ALP-induced oscillation that we seek.
  - The raw Sgr A* CCTP series is dominated by intrinsic variability on timescales longer than the putative ALP period.
  - We introduce a controlled, soft high-pass filter K to suppress slow-varying astrophysical components.
  - Estimate a smooth trend, subtract it from the raw CCTP series, and fit the residuals.

$$K(t,s) = \exp\left(-\frac{(t-s)^2}{2\sigma^2}\right)$$

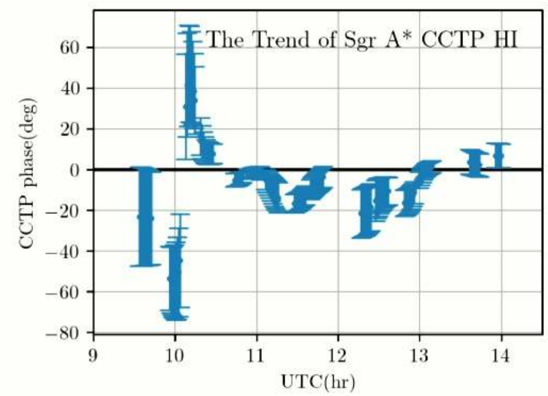

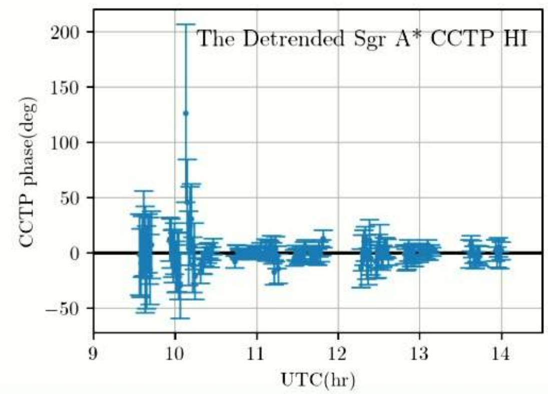

Sgr A* result

- It does not uniquely separate astrophysics from ALP physics.
- The trade-off is that high frequency intrinsic variations can still bypass this Gaussian detrending, and ALP signals can also be suppressed.
- The constraint is weaker than that of M87*, but we are the first to push the constraint at this mass range at the near-horizon scale.

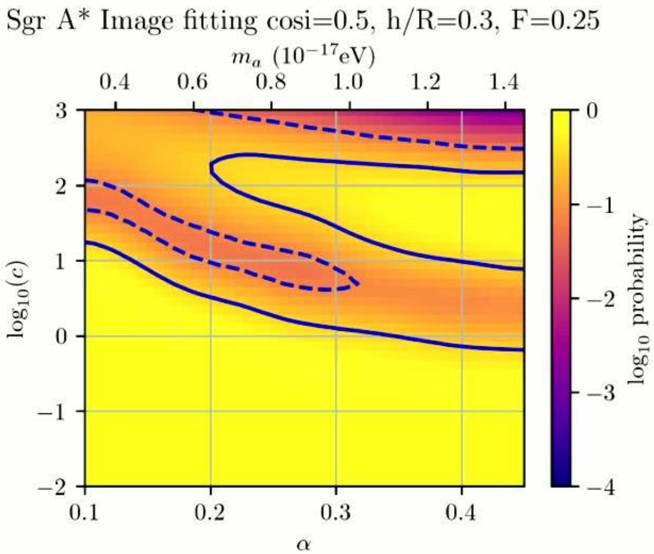

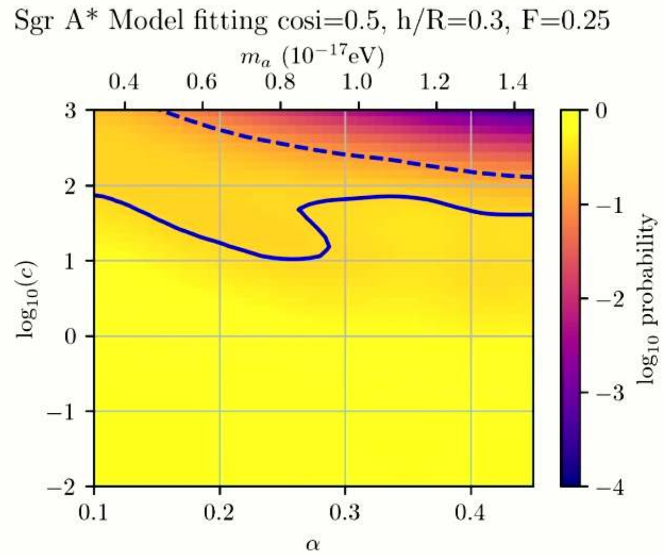

FPS N/A GPU 4% 39°C 6W CPU 12%

Final comparison: M87*, Sgr A*, and external bounds

Results

- What's the external structure/bimodality?
  - Different source morphology and nuisance parameters make the constraints different.
  - If we extract samples from the allow regions of "image" constraints, they generally fit within the CCTP errorbars. When they don't, the peaks occur mostly in temporal gaps of the EHT CCTP sampling, so it is not ruled out by the data.

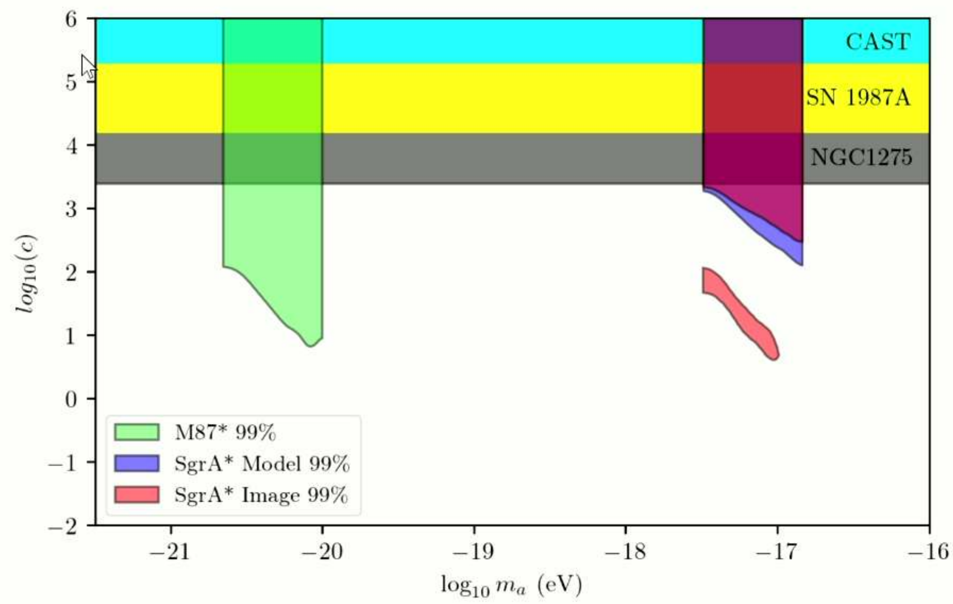

Wang & Broderick 2024, 2026; Anastassopoulos et al. 2017; Payez et al. 2015; Reynolds et al. 2020.

What limits the sensitivity, why future EHT / ngEHT will help?

1. Source variability

Cleaner sources make a coherent signal stand out. That is why M87* currently wins.

2. Polarimetric S/N

More sensitive stations and better-sampled quadrangles tighten the CCTP time series.

3. Observing Time

More data cross multiple days can also S/N.

Future arrays help in these concrete ways:

- **more stations** → more independent quadrangles, more u-v coverage
- **longer observing time** → more data to cover multiple periods
- **better polarimetric sensitivity** → smaller CCTP error bars
- **more bands** → separate plasma effects from achromatic ALP signals

Take-home messages

- Axion clouds can imprint time-dependent EVPA signatures near SMBHs.
- Closure trace / CCTP provide a robust, non-imaging observable to detect axion-induced birefringence effect.
- M87* is the clean test bed which validates our pipeline. Sgr A* is the harder but still informative extension.
- With future arrays/operations that provide more independent quadrangles and better sensitivity, we expect to push the constraints broader and deeper.

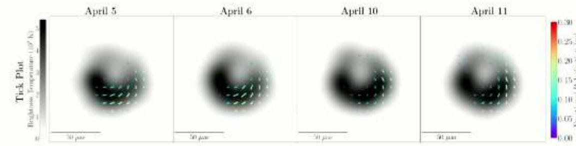

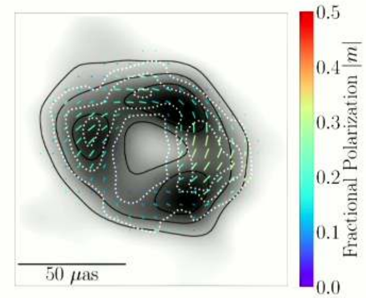

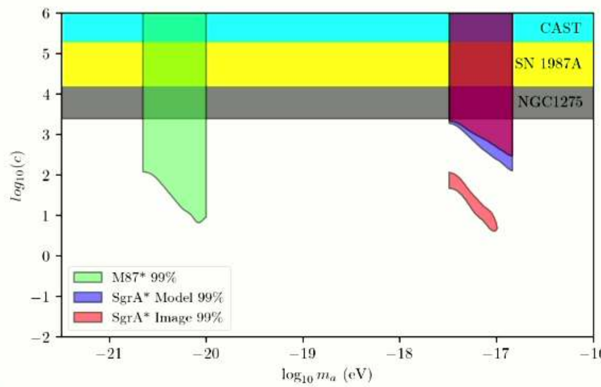

Thank you!